

Chapter 1

Monte Carlo simulation of particle transport using GORILLA

This chapter is taken without change from [?], as the author of this thesis has made contributions to this publication, appearing therefore as co-author. The content is furthermore relevant to this thesis as it gives valuable insights in the application of the code *GORILLA*.

1.1 Monte Carlo evaluation of neoclassical transport coefficients, performance benchmark

Evaluation of neoclassical transport coefficients using the Monte Carlo method [?, ?] is widely used for stellarators and tokamaks with 3D perturbations of the magnetic field [?, ?, ?, ?, ?, ?, ?]. An advantage of this method in its original, full- f form is the use of test particle guiding-center orbits without requiring model simplifications needed in (more efficient) local approaches. Therefore Monte Carlo methods provide an unbiased reference point in cases where those simplifications affect the transport such as for regimes with significant role of the tangential magnetic drift [?, ?]. An obvious disadvantage is that for realistic magnetic configurations Monte Carlo methods are CPU-intensive with most of the CPU time spent for the integration of the guiding-center motion. The application of the proposed geometric integration method for this purpose instead of the usual Runge-Kutta method results in a visible speed-up of the computations without significantly biasing the results. Here, this application is made for benchmarking purposes assuming that the inaccuracies in orbit integration which are tolerable in computations of transport coefficients are also tolerable in global modelling of macroscopic plasma parameters.

The proposed orbit integration method is applied within a standard Monte Carlo algorithm [?] using the Lorentz collision model for the evaluation of the mono-energetic radial diffusion coefficient D_{11} . The latter is determined via the average

square deviation of the normalized toroidal flux s from its starting value s_0 as follows,

$$D_{11} = \frac{1}{2t} \langle (s(t) - s_0)^2 \rangle. \quad (1.1)$$

Here, angle brackets $\langle \dots \rangle$ denote an ensemble average, $s(0) = s_0$, and the test particle tracing time t is chosen to be larger than the local distribution function relaxation time τ_{rel} and smaller than the radial transport time, $t = 10\tau_{\text{rel}}$. A Monte Carlo collision operator identical to that of Ref. [?] is applied here in-between constant collisionless orbit integration steps Δt . These steps are small enough compared to the typical bounce time τ_b and collision time τ_c ,

$$\Delta t = \min \left(\frac{\tau_b}{20}, \frac{\tau_c}{20} \right). \quad (1.2)$$

Here, $\tau_c = 1/\nu$ and $\tau_b = 2\pi R_0/(vN_{\text{tor}})$ with ν , R_0 , v and N_{tor} denoting collisional deflection frequency, major radius, particle velocity and number of toroidal field periods, respectively. The relaxation time τ_{rel} is determined as the largest of τ_c and τ_b^2/τ_c .

In the present example, the mono-energetic radial diffusion coefficient has been evaluated for the quasi-isodynamic stellarator configuration [?] used also for collisionless orbits in section III B of [?]. Guiding-center orbits were computed with the geometric integration method in symmetry flux coordinates using polynomial series solutions of various orders K . The grid size $N_s \times N_\vartheta \times N_\varphi = 100 \times 60 \times 60$ was selected to be appropriate to minimize the numerical diffusion (see the previous section.) In a reference computation, guiding-center equations (??) in symmetry flux variables with electromagnetic field interpolated by 3D cubic splines were integrated by an adaptive RK4/5 integrator. In order to minimize statistical errors, computations have been performed for a large ensemble size of 10000 particles.

The results for D_{11} computed for 3 keV electrons and ions at $s_0 = 0.6$ are presented in Fig. 1.1. Values of radial electric field E_r and deflection frequency ν , which determine transport regimes, are respectively characterized here by two dimensionless parameters [?], Mach number $v_E^* = cE_r/(vB_0)$ and collisionality $\nu^* = (R_0\nu)/(\iota v)$, where ι is the rotational transform. For the ions, in addition to the $\mathbf{E} \times \mathbf{B}$ rotation, also the tangential magnetic drift plays a significant role which can be seen from the shift of the D_{11} maximum on v_E^* dependence. The results of geometric integration stay in agreement with the reference computation within the 95 % confidence interval in all cases even for the lowest order polynomial solution $K = 2$. Therefore, as shown below, a significant gain in the computation time can be obtained in this kind of calculations.

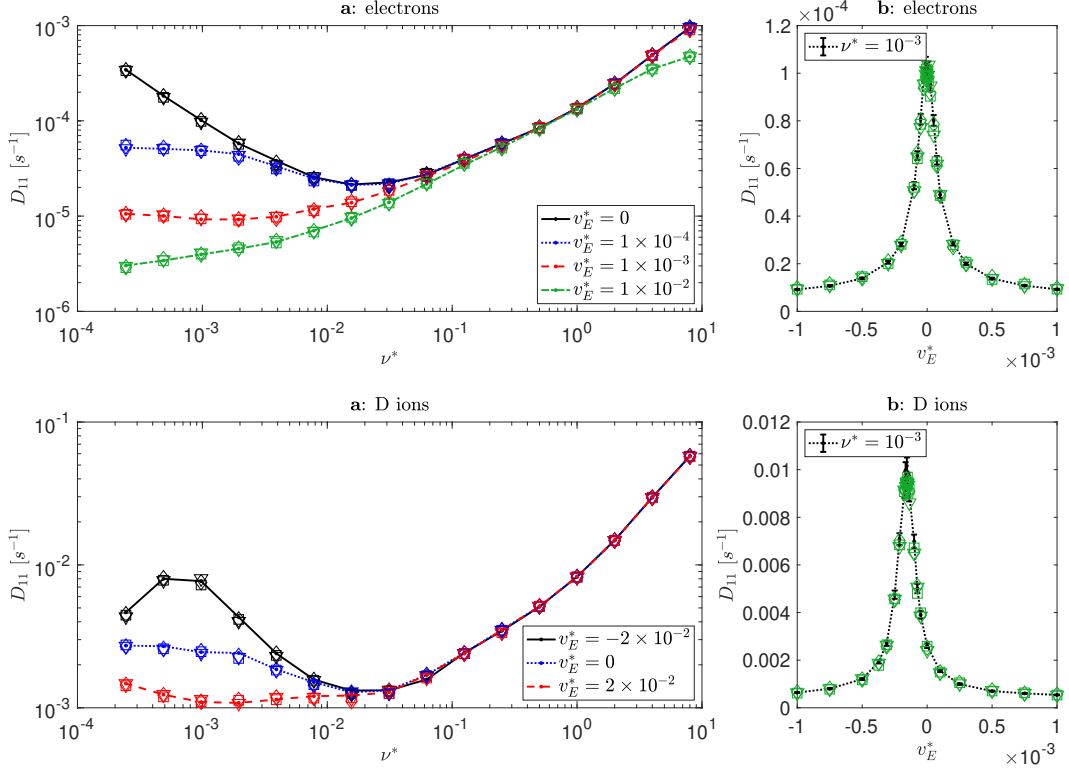


Figure 1.1: Mono-energetic radial diffusion coefficients D_{11} for electrons (top) and deuterium ions (bottom) as functions of (a) normalized collisionality ν^* and (b) Mach number v_E^* . Lines of various styles (see the legends) - reference computation, markers - results of geometric integration with polynomial solution of the order K for $K = 2$ (\diamond), $K = 3$ (\square) and $K = 4$ (∇). Error bars indicate 95 % confidence interval.

Moreover, we compare the performance and scaling for parallel computation of guiding-center orbits using the geometric orbit integration method with computations using standard reference integrators (RK4 and adaptive RK4/5). For this, different integrators have been used within D_{11} computation described above for a particular choice of dimensionless parameters, $v_E^* = 10^{-3}$ and $\nu^* = 10^{-3}$, and an increased ensemble size of 30000 test particles. The numerical experiment has been performed on a single node of the COBRA cluster of MPCDF with 40 CPU cores (Intel Xeon Gold 6126) running 80 concurrent threads with hyperthreading.

The reference value for the transport coefficient, $D_{11,\text{ref}}$, and the reference CPU time are obtained by orbit integration with an adaptive RK4/5 integrator with a relative tolerance of 10^{-9} . The accuracy of the D_{11} evaluation using different computation parameter settings is represented by the relative error $\delta D_{11}/D_{11,\text{ref}}$ where $\delta D_{11} = |D_{11} - D_{11,\text{ref}}|$. The CPU time purely used for orbit integration serves as a measure for the computational effort of the methods. This given CPU time does not contain any overhead operations, e.g. the construction of the grid, generation

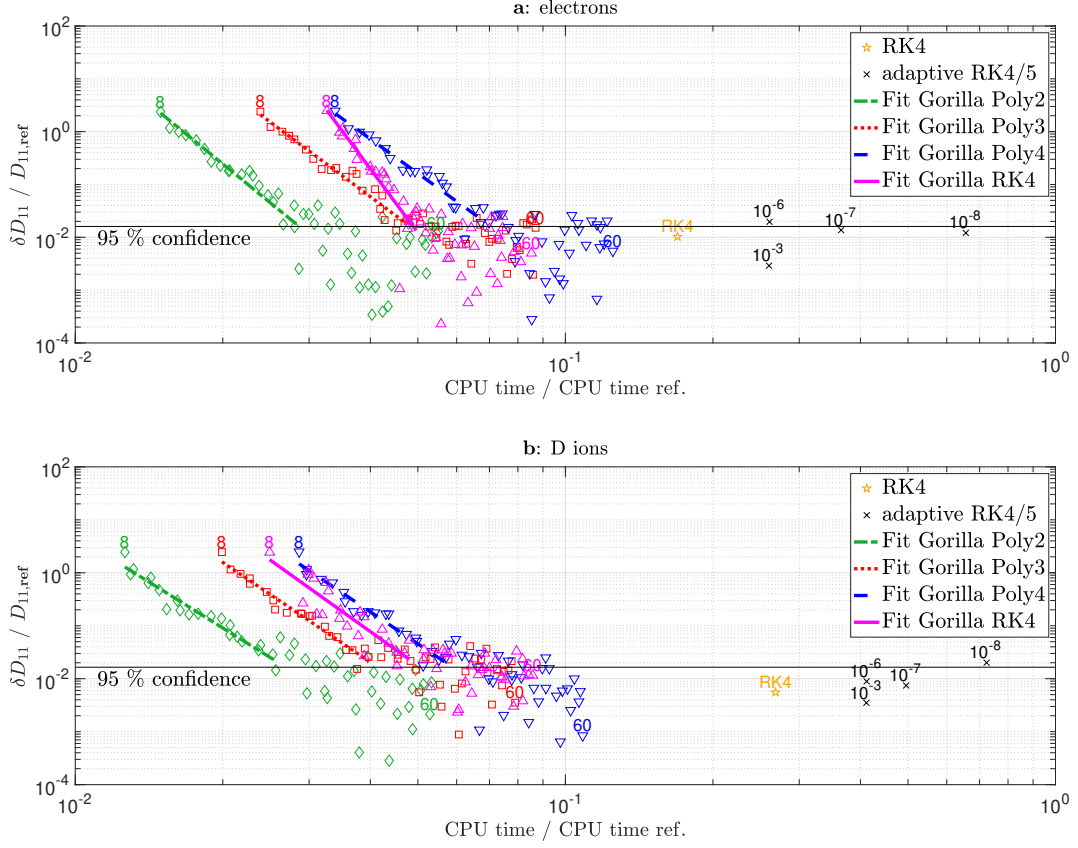


Figure 1.2: Relative error of mono-energetic radial transport coefficient D_{11} of electrons (top) and D ions (bottom) vs. relative CPU time. Compared orbit integration methods are: Runge-Kutta 4 (\star), Adaptive RK4/5 with various relative errors indicated in the plot (\times), geometric integration with polynomial solution (*GORILLA Poly*) of the order $K = 2$ (\diamond), $K = 3$ (\square) and $K = 4$ (∇), and with RK4 solution (*GORILLA RK4*, \triangle). Fits of results are depicted with lines according to the legend. Random error of the reference result, $D_{11,\text{ref}}$, is depicted as a horizontal line limiting its 95 % confidence interval.

of random numbers for pitch-angle scattering and computation of D_{11} by evaluating Eq. 1.1 with the help of a least-squares regression.

Fig. 1.2 shows the relative error of the mono-energetic radial transport coefficient versus the relative CPU time of computations using the geometric orbit integration method with the polynomial series solution of various orders, *GORILLA Poly*, and the iterative scheme with RK4 integration and Newton steps, *GORILLA RK4*. Accuracy and CPU time of geometric orbit integrations have been varied by mutually changing the angular grid size $N_\theta \times N_\varphi$ from 8×8 to 60×60 while keeping the radial grid size constant at $N_s = 100$. In the stellarator configuration of Ref. [?] used here, the number of toroidal harmonic modes per field period is 14, leading to a minimum toroidal grid size $N_\varphi = 28$ in order to satisfy the Nyquist-Shannon sampling theorem [?, ?]. Therefore, regression lines are drawn for the range of data points with grid sizes from

8×8 until 28×28 , clearly showing a convergent behavior of D_{11} with increasing grid refinement. Furthermore, the adaptive RK4/5 integration is additionally performed with relative tolerances of 10^{-3} , 10^{-6} , 10^{-7} and 10^{-8} , respectively. Note that the computational speed of the adaptive RK4/5 integration with a relative tolerance of 10^{-6} cannot be increased by higher relative tolerances, e.g. 10^{-3} , since the macroscopic Monte Carlo time step, Δt Eq. (1.2), is already elapsed within a single RK4/5 step with sufficient accuracy. Hence, also the non-adaptive Runge-Kutta 4 method is tested, which naturally needs one field evaluation less per time step than RK4/5. In all cases, the relative error of RK4/5 and Runge-Kutta 4 results is determined here mainly by statistical deviations, with a random error dominating the bias.

Besides statistical errors due to Monte Carlo sampling, a limit for capturing all toroidal and poloidal field harmonics is given by a minimum grid size of two points per period due to the Nyquist–Shannon sampling theorem. Fig. 1.2 visibly shows that statistical fluctuations already dominate the bias of all variants of the geometric integration method above this sampling threshold, despite the large ensemble size of 30000 particles. To avoid possible sampling artifacts at even higher higher particle count, we consider the geometric orbit integration method at the toroidal grid size N_φ of at minimum twice the number of toroidal modes in the magnetic field configurations. The variant with the polynomial series solution truncated at $K = 2$ (*GORILLA Poly 2*) at this grid resolution can be considered the fastest sufficiently accurate tested method to compute D_{11} for thermal ions and electrons. In case of D ions with an energy of 3 keV this method is one order of magnitude faster than the Runge-Kutta 4 integrator which is the fastest reference method.